A Distribution of mutation effects on fitness

In the two environments, mutations occur at rate U and create independent and identically distributed (iid) random variations $\mathbf{dx}$ around the phenotype of the parent, for each trait. We assumed here a standard Gaussian distribution of the mutation phenotypic effects (Kimura, 1965; Lande, 1980): $\mathbf{dx} \sim \mathcal{N}(0, \lambda I_n)$, where λ is the mutational variance at each trait, and I_n is the identity matrix in n dimensions. These assumptions induce a distribution of the mutation effects on fitness, given the relative fitness $m_p \leq 0$ of the parent. This distribution has stochastic representation (Martin, 2014)

$$s \sim -\, m_p - \frac{\lambda}{2}\chi^2_n\left(-\, 2\, m_p/\lambda\right),$$

where $\chi^2_n\left(-\, 2\, m_p/\lambda\right)$ denotes the noncentral chi-square distribution with n degrees of freedom and noncentrality $-2\, m_p/\lambda$. This distribution is detailed elsewhere (reviewed in Tenaillon, 2014), its mean is $\mathbb{E}[s] = -n\, \lambda/2$. Alternatively, it can be characterized by its moment generating function:

$$\mathbb{E}[e^{s\, z}|m_p] = M_*(z)\, e^{\omega(z)\, m_p}, \tag{A1}$$

with

$$M_*(z) = \frac{1}{(1+\lambda\, z)^{n/2}} \text{ and } \omega(z) = \frac{-\lambda\, z^2}{1+\lambda\, z}. \tag{A2}$$

B Fitness distribution of the migrants: derivation of formula (3)

Consider an individual with phenotype $\mathbf{x}$. Its fitness in the source is

$$m_{source} = -\|\mathbf{x} - \mathbf{x}^\star\|^2/2,$$

where $\mathbf{x}^\star$ is the optimal phenotype in the source, whereas its fitness in the sink is $m_{migr} = -\|\mathbf{x}\|^2/2$. We observe that

$$\begin{aligned} m_{migr} &= -\frac{\|\mathbf{x} - \mathbf{x}^\star + \mathbf{x}^\star\|^2}{2} \\ &= -\frac{\|\mathbf{x} - \mathbf{x}^\star\|^2 + \|\mathbf{x}^\star\|^2 + 2(\mathbf{x} - \mathbf{x}^\star)\cdot\mathbf{x}^\star}{2} \\ &= m_{source} - \frac{\|\mathbf{x}^\star\|^2}{2} - \|\mathbf{x} - \mathbf{x}^\star\|\ \|\mathbf{x}^\star\| u \\ &= m_{source} - m_D - 2\sqrt{m_D|m_{source}|}u, \end{aligned} \tag{A3}$$

with $m_D = \|\mathbf{x}^\star\|^2/2$ and a constant $u \in [-1, 1]$. As the source is assumed to be at the mutation-selection equilibrium, the distribution of fitness in the source satisfies $m_{source} \sim -\Gamma(n/2, \mu)$ (Martin and Roques, 2016, equation (10)) and the corresponding moment generating function is $M_{m_{source}}(z) = (1 + \mu z)^{-n/2}$. The results in (Martin and Lenormand, 2015) show that u is a random variable with moment generating function:

$$M_u(z) := \mathbb{E}[e^{uz}] = {}_0F_1(n/2,\ z^2/4),$$

with ${}_0F_1$ the hypergeometric function, defined by ${}_0F_1(\theta, z) = \sum_{k=0}^{\infty} \frac{1}{\theta(\theta+1)\cdots(\theta+k-1)}\ \frac{z^k}{k!}$. Let us first compute the moment generating function $M_{migr}(z) := \mathbb{E}[e^{m_{migr}z}]$. We have

$$M_{migr}(z) = \mathbb{E}[\mathbb{E}[e^{m_{migr}z}|m_{source}]],$$

and using (A3),

$$\begin{aligned} M_{migr}(z) &= \mathbb{E}\left[e^{m_{source}z} M_u\left(-2\sqrt{m_D|m_{source}|}z\right)\right] e^{-m_D z} \\ &= \mathbb{E}\left[e^{m_{source}z}\ {}_0F_1\left(n/2,\ -m_D m_{source} z^2\right)\right] e^{-m_D z}. \end{aligned}$$

Thanks to the definition of the hypergeometric function ${}_0F_1(n/2, z)$, we get:

$$\begin{aligned} M_{migr}(z) &= \sum_{k=0}^{\infty} \frac{(-m_D)^k}{n/2(n/2+1)\cdots(n/2+k-1)}\ \frac{z^{2k}}{k!}\mathbb{E}[e^{m_{source}z} m_{source}^k] e^{-m_D z} \\ &= \sum_{k=0}^{\infty} \frac{(-m_D)^k}{n/2(n/2+1)\cdots(n/2+k-1)}\ \frac{z^{2k}}{k!} M^{(k)}_{m_{source}}(z) e^{-m_D z}, \end{aligned}$$

with $M^{(k)}_{m_{source}}(z)$ the k$^{\text{th}}$ derivative of $M_{m_{source}}(z)$ with respect to z. Thus,

$$\begin{aligned} M_{migr}(z) &= \sum_{k=0}^{\infty} \frac{1}{k!} \left(\frac{m_D \mu z^2}{1+\mu z} \right)^k (1+\mu z)^{-n/2} e^{-m_D z} \\ &= \frac{1}{(1+\mu z)^{n/2}} \cdot \exp\left[-m_D z + \frac{m_D \mu z^2}{1+\mu z} \right]. \end{aligned}$$

Setting $\phi(z) = \ln\left(M_{migr}(z)\right)$, we obtain formula (3).

Let us now show give the distribution of the migrants in the sink. Let p_{migr} be defined by:

$$p_{migr}(m) = \begin{cases} \frac{1}{\mu} \left(\frac{|m|}{m_D} \right)^{\frac{1}{2}\left(\frac{n}{2}-1\right)} e^{\frac{m-m_D}{\mu}} I_{\frac{n}{2}-1}\left[\frac{2\sqrt{m_D|m|}}{\mu} \right], \text{ if } m < 0 \\ 0, \text{ if } m \geq 0 \end{cases}, \qquad \text{(A4)}$$

where I_ν is the modified Bessel function of the first kind. We just have to check that the moment generating function of p_{migr} is M_{migr}:

$$\begin{aligned} \int_{-\infty}^{0} e^{zx} p_{migr}(x) dx &= \int_{-\infty}^{0} e^{zx} \frac{1}{\mu} \left(\frac{|x|}{m_D} \right)^{\frac{n/2-1}{2}} e^{\frac{x-m_D}{\mu}} I_{\frac{n}{2}-1}\left[\frac{2\sqrt{m_D|x|}}{\mu} \right] dx \\ &= e^{-m_D/\mu} \int_{-\infty}^{0} \sum_{p=0}^{\infty} e^{(z+1/\mu)x} \frac{m_D^p}{\mu^{2p+n/2}} \cdot \frac{1}{p!} \cdot \frac{|x|^{p+n/2-1}}{\mathbf{\Gamma}(p+n/2)} dx \\ &= e^{-m_D/\mu} \sum_{p=0}^{\infty} \frac{m_D^p}{\mu^{2p+n/2}} \cdot \frac{1}{p!} \cdot \frac{1}{\mathbf{\Gamma}(p+n/2)} \int_{-\infty}^{0} e^{(z+1/\mu)x} |x|^{p+n/2-1} dx, \end{aligned}$$

where I_ν is the modified Bessel function of the first kind and $\mathbf{\Gamma}$ the gamma function.

Now, for all positive numbers a and b, we have:

$$\int_{-\infty}^{0} e^{ax} |x|^{b-1} dx = \frac{1}{a^b} \int_{0}^{\infty} e^{-x} |x|^{b-1} dx = \frac{\mathbf{\Gamma}(b)}{a^b}.$$

Therefore, we get, for $z > -1/\mu$:

$$\begin{aligned} \int_{-\infty}^{0} e^{zx} p_{migr}(x) dx &= e^{-m_D/\mu} \sum_{p=0}^{\infty} \frac{m_D^p}{\mu^{2p+n/2}} \cdot \frac{1}{p!} \cdot \frac{1}{\mathbf{\Gamma}(p+n/2)} \frac{\mathbf{\Gamma}(p+n/2)}{(z+1/\mu)^{p+n/2}} \\ &= \frac{e^{-m_D/\mu}}{(1+\mu z)^{n/2}} \sum_{p=0}^{\infty} \left(\frac{m_D/\mu}{1+\mu z} \right)^p \cdot \frac{1}{p!} \\ &= \frac{e^{-m_D/\mu}}{(1+\mu z)^{n/2}} \exp\left(\frac{m_D/\mu}{1+\mu z} \right) \\ &= \frac{1}{(1+\mu z)^{n/2}} \exp\left(-\frac{m_D z}{1+\mu z} \right). \end{aligned}$$

This is consistent with formula (3), which proves that the for p_{migr} is correct.

C PDE satisfied by the CGF of the fitness distribution

In the WSSM regime, and in the absence of immigration, Martin and Roques (2016) (see Appendix E, equation (E5)) have shown that the CGF of the fitness distribution satisfies the following equation:

$$\partial_t C_t(z) = \partial_z C_t(z) - \partial_z C_t(0) - \mu^2 \left(z^2 \, \partial_z C_t(z) + \frac{n}{2} z \right), \; z \geq 0.$$

We derive here the additional term in (6), which describes the effect of immigration on the CGF.

In that respect, we consider a discrete population of size $N(t) \in \mathbb{N}$ at time t, and the corresponding fitnesses $(m_1(t), \ldots, m_{N(t)}(t))$. We define the "empirical" moment generating function

$$M_t(z) := \frac{1}{N(t)} \sum_{i=1}^{N(t)} e^{m_i(t)\, z}.$$

Assuming a Poisson number of immigration events, with rate d per unit time (see Section 2.5), for Δt small enough, the probability that a single immigration events occurs during $(t, t+\Delta t)$ is approximately $d\,\Delta t$. The probability that several immigration events occur during this time interval is close to 0. Therefore, the expected change in the moment generating function during Δt, conditionally on the fitness m_{migr} of the unique migrant, is:

$$\begin{aligned}
\Delta M_t(z|m_{migr}) &= d\ \Delta t \left[\frac{1}{N(t)+1} \left(\sum_{i=1}^{N(t)} e^{m_i(t)\ z} + e^{m_{migr}\ z} \right) - \frac{1}{N(t)} \sum_{i=1}^{N(t)} e^{m_i(t)\ z} \right] \\
&= d\ \Delta t \left[\frac{e^{m_{migr}\ z}}{N(t)+1} - \frac{M_t(z)}{N(t)+1} \right].
\end{aligned}$$

Taking expectation over the distribution of m_{migr} (see Appendix B for more details on the distribution of m_{migr}), we get

$$\Delta M_t(z) = \frac{d\ \Delta t}{N(t)+1} \left(e^{\phi(z)} - M_t(z) \right),$$

with $\phi(z) = \ln\left(\mathbb{E}\left[e^{m_{migr}\ z}\right]\right)$. The corresponding change in the CGF $C_t(z) = \ln M_t(z)$ is $\Delta C_t(z) \approx \Delta M_t(z)/M_t(z)$. Thus,

$$\Delta C_t(z) \approx \frac{d\ \Delta t}{N(t)} \left(e^{\phi(z) - C_t(z)} - 1 \right).$$

Finally, dividing the above expression by Δt and passing to the limit $\Delta t \to 0$, we obtain the last term in (6), which describes the effect of immigration on the CGF:

$$\frac{d}{N(t)} \left(e^{\phi(z) - C_t(z)} - 1 \right). \tag{A5}$$

D Solution of the system (1) & (6)

This section is devoted to the mathematical study of the system (1) & (6). We rewrite it in the following form:

$$\begin{cases} \partial_t C_t(z) = \alpha(z)\partial_z C_t(z) - \overline{m}(t) + \beta(z) + \frac{d}{N(t)}\left(e^{\phi(z)-C_t(z)} - 1\right), \\ N'(t) = N(t)\ (r_{\max} + \overline{m}(t)) + d, \\ C_t(0) = 0, \\ N(0) = 0, \end{cases} \tag{A6}$$

with $t > 0$ and $z \geq 0$, and where $\overline{m}(t) = \partial_z C_t(0)$, $d \geq 0$, $\alpha(z) := 1 - \mu^2\ z^2$, $\beta(z) := -\mu\, n\, z/2$.

We can easily check that the sink is not empty at each time $t > 0$:

Lemma 1. *Assume that $\overline{m}$ is continuous over $[0, \infty)$. Then, at all time $t > 0$, we have $N(t) > 0$.*

Proof. For $\varepsilon > 0$ small enough, as $N'(0) = d > 0$, we have $N(t) > 0$ for all $t \in (0, \varepsilon]$. Additionally, for all $t \geq \varepsilon$,

$$N(t) = e^{\int_\varepsilon^t (r_{\max} + \overline{m}(s))\, ds} \left(N(\varepsilon) + d \int_\varepsilon^t e^{-\int_\varepsilon^v (r_{\max} + \overline{m}(s))\, ds}\, dv \right) > 0. \tag{A7}$$

□

Let $N(t)$, $C_t(z)$ be a solution of (A6), such that $\overline{m}$ is continuous over $[0, \infty)$. Set $D_t(z) = C_t(y(z))$, with $y(z) = \tanh(\mu z)/\mu$ which satisfies:

$$\begin{cases} y'(z) = \alpha(y(z)), \\ y(0) = 0, \end{cases}$$

so that

$$\partial_t D_t(z) = \partial_t C_t(y(z)) \ \text{ and } \ \partial_z D_t(z) = \alpha(y(z))\partial_z C_t(y(z)).$$

Thus, $D_t(z)$ satisfies the simpler equation

$$\partial_t D_t(z) = \partial_z D_t(z) - \overline{m}(t) + \beta(y(z)) + \frac{d}{N(t)}\left(e^{\phi(y(z))-D_t(z)} - 1\right),$$

with $\overline{m}(t) = \partial_z D_t(0)$.

Using the method of characteristics, we derive an analytic expression for $D_t(z)$. Fix $z \geq 0$ and denote for all $z \geq t > 0$:

$$v(t) = \exp(D_t(z - t)).$$

The function $v \in C^1((0,z])$ satisfies for all $t \in (0,z)$:

$$\begin{aligned} v'(t) &= \left(\partial_t D_t(z-t) - \partial_z D_t(z-t)\right) v(t), \\ &= \left[\beta(y(z-t)) - \overline{m}(t) - \frac{d}{N(t)}\right] v(t) + \frac{d}{N(t)}\, e^{\phi(y(z-t))}, \\ &= \left[\beta(y(z-t)) - \frac{N'(t)}{N(t)} + r_{\max}\right] v(t) + \frac{d}{N(t)}\, e^{\phi(y(z-t))}, \end{aligned}$$

thanks to $N'(t) = (r_{\max} + \overline{m}(t))N(t) + d$. Let us fix times $0 < \varepsilon < t$. By Lemma 1, we know that $N(s) > 0$, for all $s \in [\varepsilon, t]$ and so $v(t)$ is given by:

$$\begin{aligned} v(t) = \exp &\left[\int_\varepsilon^t \left(\beta(y(z-\tau)) - \frac{N'(\tau)}{N(\tau)} + r_{\max}\right) d\tau\right] \\ &\left[e^{C(\varepsilon, y(z))} + \int_\varepsilon^t \frac{d\; e^{\phi(y(z-\tau))}}{N(\tau)} \exp\left(-\int_\varepsilon^\tau \left(\beta(y(z-s)) - \frac{N'(s)}{N(s)} + r_{\max}\right) ds\right) d\tau\right]. \end{aligned}$$

As $\int_\varepsilon^t \frac{N'(s)}{N(s)} ds = \ln N(t) - \ln N(\varepsilon)$, we can simplify the last expression to:

$$\begin{aligned} v(t) = \exp &\left[-\ln N(t) + \int_\varepsilon^t \left(\beta(y(z-\tau)) + r_{\max}\right) d\tau\right] \\ &\left[N(\varepsilon) \ln e^{C(\varepsilon, y(z))} + \int_\varepsilon^t d\; e^{\phi(y(z-\tau))} \exp\left(-\int_\varepsilon^\tau \left(\beta(y(z-s)) + r_{\max}\right) ds\right) d\tau\right]. \end{aligned}$$

Taking the limit as ε tends to 0 and using the fact that the initial population in the sink is $N(0) = 0$, the above expression can be simplified to:

$$v(t) = d \int_0^t e^{\phi(y(z-\tau)) - \int_0^\tau (\beta(y(z-s)) + r_{\max}) ds} d\tau \cdot \exp\left[-\ln N(t) + \int_0^t \left(\beta(y(z-\tau)) + r_{\max}\right) d\tau\right].$$

Hence, by reversing the characteristics, we get:

$$\begin{aligned} D_t(z) = \int_0^t \beta(y(z+\tau)) d\tau - \ln\left(N(t)\right) + r_{\max} t \\ + \ln\left[d \int_0^t e^{\phi(y(z+\tau)) - r_{\max}(t-\tau) - \int_\tau^t \beta(y(z+s)) ds} d\tau\right]. \end{aligned}$$

This leads to an explicit but complex formula for $C_t(z)$ thanks to the relation

$$C_t(z) = D_t\left(\frac{1}{\mu} \mathrm{atanh}(\mu z)\right). \tag{A8}$$

Additionally, we have:

$$\partial_z D_t(z) = \beta(y(z+t)) - \beta(y(z)) + \frac{\int_0^t \partial_z\, g(t,z,\tau)\, d\tau}{\int_0^t g(t,z,\tau)\, d\tau},$$

with $g(t,z,\tau) = \exp\left[\phi(y(z+\tau)) + r_{\max}(\tau - t) - \int_\tau^t \beta(y(z+s))ds\right]$. Using the fact that $\overline{m}(t) = \partial_z D_t(0)$, $y(0) = 0$ and $\beta(0) = 0$, we get:

$$\begin{aligned}
\overline{m}(t) =& \beta(y(t)) + \frac{\int_0^t g(t,0,\tau)\ \left[y'(\tau)\phi'(y(\tau)) + \beta(y(\tau)) - \beta(y(t))\right]\ d\tau}{\int_0^t g(t,0,\tau)\, d\tau},\\
=& \frac{\int_0^t g(t,0,\tau)\ \left[y'(\tau)\phi'(y(\tau)) + \beta(y(\tau))\right]\ d\tau}{\int_0^t g(t,0,\tau)\, d\tau},\\
=& \frac{\int_0^t g(t,0,\tau)\ \left[y'(\tau)\phi'(y(\tau)) + \beta(y(\tau)) + r_{\max}\right]\ d\tau}{\int_0^t g(t,0,\tau)\, d\tau} - r_{\max},\\
=& \frac{\int_0^t g(t,0,\tau)\, \partial_\tau g(t,0,\tau)\, d\tau}{\int_0^t g(t,0,\tau)\, d\tau} - r_{\max},\\
=& \frac{g(t,0,t) - g(t,0,0)}{\int_0^t g(t,0,\tau)\, d\tau} - r_{\max}.
\end{aligned}$$

Using the expression $g(t,0,\tau) = \exp\left[\phi(y(\tau)) + r_{\max}(\tau - t) - \int_\tau^t \beta(y(s))ds\right]$, the formula (3) for ϕ and $y(z) = \tanh(\mu z)/\mu$, we finally get:

$$\overline{m}(t) = \frac{\exp\left[(r_{\max} - \mu\,\frac{n}{2})t + \frac{m_D}{2\mu}\,(e^{-2\mu t} - 1)\right] - 1}{\int_0^t \exp\left[(r_{\max} - \frac{n}{2}\mu)\tau + \frac{m_D}{2\mu}\,(e^{-2\mu\tau} - 1)\right] d\tau} - r_{\max}. \tag{A9}$$

As we have an explicit formula for $\overline{m}(t)$, we can also solve the ODE $N'(t) = N(t)\,(r_{\max} + \overline{m}(t)) + d$ (formula (A7), with $\varepsilon = 0$ and $N(\varepsilon) = 0$). Finally, we can check that $N(t)$, $C_t(z)$ (defined by (A8)) is a solution of (A6) such that $\overline{m}$ (given by (A9)) is continuous over $[0,\infty)$. Using the expression (A9) with $\overline{r}(t) = r_{\max} + \overline{m}(t)$, we obtain the formula (7) in the main text.

E Trajectories of mean fitness: $U < U_c$

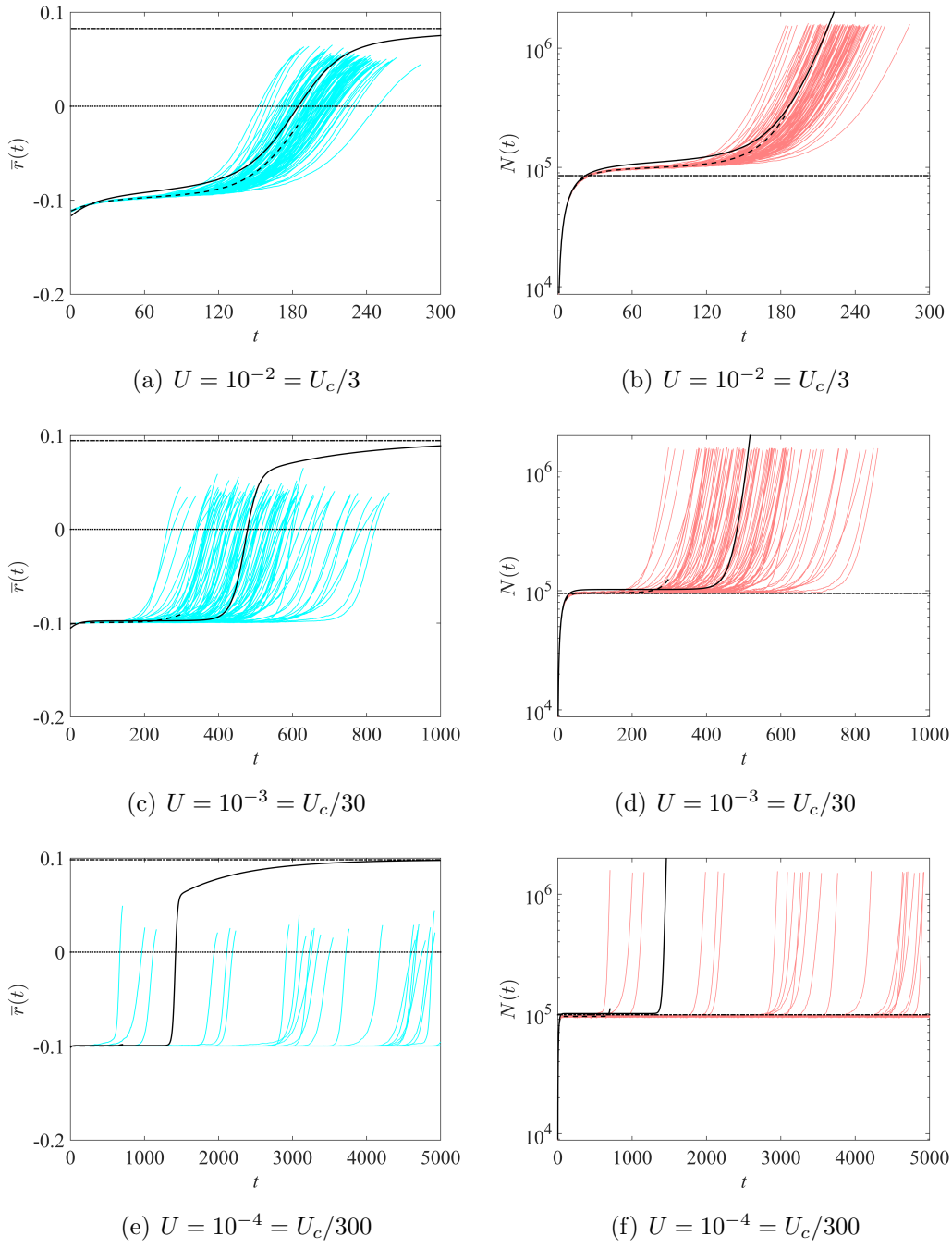

(a) $U = 10^{-2} = U_c/3$ (b) $U = 10^{-2} = U_c/3$

(c) $U = 10^{-3} = U_c/30$ (d) $U = 10^{-3} = U_c/30$

(e) $U = 10^{-4} = U_c/300$ (f) $U = 10^{-4} = U_c/300$

Figure A1: **Trajectories of mean fitnesses and population sizes, low mutation rates.** Same legend as in Fig. 2. Other parameter values are $m_D = 0.2$, $r_{\max} = 0.1$, $\lambda = 1/300$, $n = 6$ and $d = 10^4$, leading to $U_c = 0.03$.

F Range of validity of the model

We explored the range of validity of the analytical model by comparing theory and simulations over a wide range of parameter values. The raw results are given in Appendix J. Overall, the model tends to be more accurate as U and d increase and m_D (equivalently, $r_D = m_D - r_{\max}$), n and λ decrease. More precisely, theoretical and numerical analysis yield two necessary conditions for the accuracy of the model: (i) $U \geq U_c = n^2\lambda/4$, for the WSSM to apply; (ii) $dU/r_D \gg 1$, for the large d approximation to apply.
Below we detail each criterion, their robustness and possible empirical insight on their realism.

Criterion (i): it is formally derived in Appendix F of (Martin and Roques, 2016) and guarantees that the mutation term associated with the FGM linearizes to produce an analytically tractable PDE. While the model is indeed fairly accurate whenever $U > U_c$, it remains reasonably so even at fairly lower mutation rates. Even for mutation rates $U = U_c/30$ (but keeping a large d), $\overline{r}(t)$ and $N(t)$ from eq. (7) still approximately captures the average trajectories (Fig. A1, Appendix E), although the length of Phase 2 in the numerical simulations becomes more variable, around this average, as U is decreased. Consistently, Fig. 6b shows that the invasion time in eq. (9) still approximately captures the average of simulations far below $U = U_c$, with larger variability around this mean as U decreases.

As an example, empirical estimates in *E. coli*, based on a recent mutation accumulation experiment (Trindade et al., 2010) suggest $U \in [0.004, 0.006]$ and $\mathbb{E}[s] = n\lambda/2 \in [0.02, 0.04]$ (mean effect of mutations on fitness), which yields $U/U_c \in [0.2, 0.6]$ for $n = 1$ and $U/U_c \in [0.033, 0.1]$ for $n = 6$. This suggests that *E. coli* may lie somewhere below the critical mutation rate, at a similar order. Note however that estimates of these quantities are fairly scarce (even in this well studied biological model) and seem to vary substantially across experiments (medium, strain, growth conditions). We suspect that viruses (especially RNA viruses) may lie well within $U \geq U_c$, while bacteria may vary widely around $U = U_c$. Obviously any proper statement on this issue would require a full review of empirical estimates (appropriately scaled in consistent time units), wherever available.

Criterion (ii): this criterion, which is confirmed by the simulations in Appendix J and Fig. 6 panels (a) and (c), stems from the following argument: the early population size in the sink is of order $N(t) \approx d/|\overline{r}(0)|$ (no evolution), with $|\overline{r}(0)| = |r_D + \mu\, n/2| \approx r_D$ (when $\mu \ll r_D$). Thus whenever $d \gg r_D/U$, the mutant input $N(t)U$ in the sink population quickly reaches a large value $N(t)\, U \approx d\, U/r_D \gg 1$ and only increases later

on. Adaptive evolution can then take place within the sink, in a way that is captured by a deterministic approximation. Conversely, when d is smaller and/or r_D is larger, the early population size in the sink is small, so that the deterministic approximation does not apply anymore. In this case, we see that the time t_0 is much more variable, and increases on average with smaller d and larger r_D (or equivalently m_D), see Fig. 6.

Empirically evaluating the criterion (ii) requires estimates of d, U, r_D on the same timescale (hours, days, generations) in a well defined sink. Such estimates should be possible from dedicated experiments controlling the immigration rate, in strains with known mutational parameters, and environmental stresses with well characterized demographic effect. They would greatly help our understanding of source-sink dynamics. However, to the best of our knowledge, they are not available to date.

G Phenotype distribution in the sink: dynamics of $\overline{r}(t)$ and $N(t)$

The dynamics of mean fitness and population size corresponding to Fig. 3 are plotted in Fig. A2, to illustrate the occurrence of the four phases in this particular simulation.

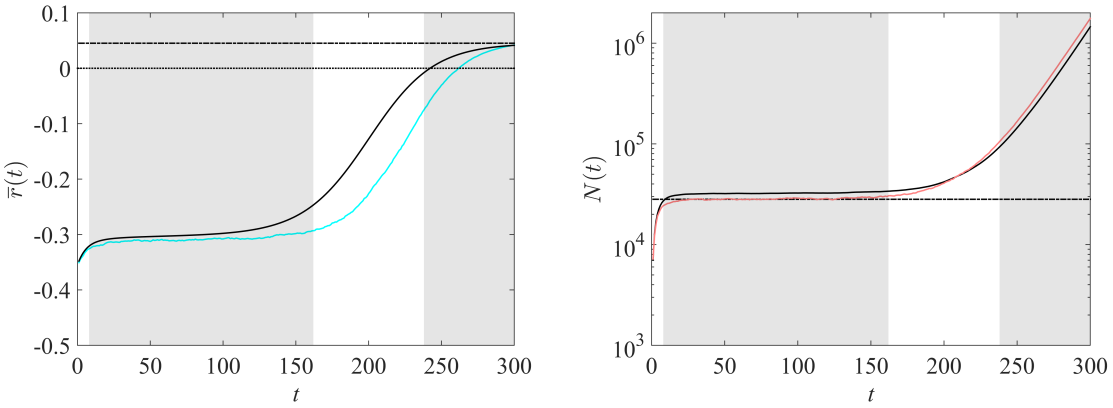

(a) (b)

Figure A2: **Trajectory of mean fitness and population size in the sink corresponding to the phenotype distribution in Fig. 3.** Same legend as in Fig. 2.

H Independence of the evolutionary dynamics with respect to the immigration rate

The value of $\overline{r}(t)$ in formula (7) does not depend on d. Thus, only the population size dynamics are influenced by the immigration rate, but not the dynamics of adaptation. Actually, this phenomenon appears for a more general deterministic black-hole sink model, with a stable source and a constant immigration rate $d \geq 0$. In the sink, we have just to assume that the environment is initially empty ($N(0) = 0$), that both demography and evolution are density-independent (so that density dependence only arises in the migration effect). Apart from that, the proposed generalization may accommodate arbitrary forms of mutation and selection effects (possibly with changes in m_D over time). The model then takes the following general form:

$$\begin{cases} \partial_t C_t(z) = \text{Selection}(t, z, C_t(z)) + \text{Mutation}(t, z, C_t(z)) + \frac{d}{N(t)} \left(e^{\phi(z) - C_t(z)} - 1 \right), \\ N'(t) = N(t)\ \overline{r}(t) + d, \\ C_t(0) = 0, \\ N(0) = 0, \end{cases}$$

with $\overline{r}(t) = \partial_z C_t(0)$ the coefficient of the exponential growth. Setting $P(t) = N(t)/d$, we observe that the above system can be written in the form:

$$\begin{cases} \partial_t C_t(z) = \text{Adaptation}(t, z, C_t(z)) + \text{Mutation}(t, z, C_t(z)) + \frac{1}{P(t)} \left(e^{\phi(z) - C_t(z)} - 1 \right), \\ P'(t) = P(t)\ \overline{r}(t) + 1, \\ C_t(0) = 0, \\ P(0) = 0, \end{cases}$$

with $\overline{r}(t) = \partial_z C_t(0)$. As this system does not depend on d, this implies that the dynamics of $P(t)$, of mean fitness $\overline{r}(t)$, and even of the full fitness distribution $(C_t(z))$ are all independent of d.

I Large time behavior of $\overline{r}(t)$

We recall that, according to formula (7),

$$\overline{r}(t) = \frac{f(t)-1}{\int_0^t f(\tau)\,d\tau},$$

with $f(t) = \exp\left[\left(r_{\max} - \mu\,\frac{n}{2}\right)t + \frac{m_D}{2\,\mu}(e^{-2\,\mu\,t}-1)\right]$.

We first show that $\overline{r}(t)$ is an increasing function of t. First, we can check that

$$f'(t) = f(t)\,\left(r_{\max} - \frac{\mu n}{2} - m_D e^{-2\mu t}\right).$$

Second, we have

$$\begin{aligned}\overline{r}'(t) &= \frac{f'(t)}{\int_0^t f(\tau)d\tau} - \frac{f(t)-1}{\left(\int_0^t f(\tau)d\tau\right)^2}\,f(t)\\ &= \frac{f(t)}{\left(\int_0^t f(\tau)d\tau\right)^2}\,\left[\left(r_{\max} - \frac{\mu n}{2} - m_D e^{-2\mu t}\right)\int_0^t f(\tau)d\tau - (f(t)-1)\right].\end{aligned}$$

Let $h(t) = \left(r_{\max} - \frac{\mu n}{2} - m_D e^{-2\mu t}\right)\int_0^t f(\tau)d\tau - (f(t)-1)$. Thus we see that

$$h'(t) = 2\,\mu\,m_D\,e^{-2\mu t}\int_0^t f(\tau)d\tau \geq 0.$$

Therefore for all $t>0$, $h(t) > h(0) = 0$, which shows that $\overline{r}$ is increasing.

Since $\overline{r}(0) = r_{\max} - \mu\,n/2 - m_D$, this implies that $\overline{r}(t) > r_{\max} - \mu\,n/2 - m_D$ for all $t>0$. In particular, $\overline{r}(\infty) \geq r_{\max} - \mu\,n/2 - m_D$ which implies that $\delta(m_D) < m_D$ in (8).

Next, we compute the limit of $\overline{r}(t)$ as $t\to\infty$.
Case (i): we assume that $r_{\max} - \mu n/2 > 0$. Then, $f(t) \sim e^{-\frac{m_D}{2\,\mu}}\,e^{(r_{\max}-\mu n/2)t}$ and

$$\int_0^t f(\tau)\,d\tau \sim e^{-\frac{m_D}{2\,\mu}}\,\frac{e^{(r_{\max}-\mu n/2)t}}{r_{\max}-\mu n/2},\ \text{as } t\to\infty.$$

Thus,

$$\overline{r}(t) \to r_{\max} - \mu n/2 \text{ as } t\to\infty.$$

Case (ii): we assume that $r_{\max} - \mu n/2 = 0$. Then $f(t) = \exp\left[\frac{m_D}{2\mu}\left(e^{-2\mu t} - 1\right)\right]$ and $\int_0^t f(\tau)\, d\tau \sim t\, e^{-m_D/(2\mu)}$ as $t \to \infty$. Thus,

$$\overline{r}(t) \sim \frac{e^{-m_D/(2\mu)} - 1}{e^{-m_D/(2\mu)} t} \to 0 \text{ as } t \to \infty.$$

Case (iii): we assume that $r_{\max} - \mu n/2 < 0$. Consider an arbitrary constant $\alpha \in (0, 2)$. We can check that, for all $t < T_\alpha := \frac{1}{2\mu} \ln \frac{2}{\alpha}$, we have:

$$e^{-2\mu t} < 1 - \alpha \mu t.$$

In the sequel, we denote $X := r_{\max} - \mu n/2$. We get:

$$\begin{aligned}
\int_0^\infty f(t)dt &= \int_0^{T_\alpha} f(t)dt + \int_{T_\alpha}^\infty f(t)dt \\
&\leq \int_0^{T_\alpha} \exp\left((X - m_D \alpha/2)t\right) dt \\
&+ \int_{T_\alpha}^\infty \exp\left[Xt + \frac{m_D}{2\mu}\left(e^{-2\mu T_\alpha} - 1\right)\right] dt.
\end{aligned}$$

Using the assumption $X = r_{\max} - \mu n/2 < 0$, we obtain:

$$\int_0^\infty f(t)dt \leq \frac{e^{(X - m_D \alpha/2) T_\alpha} - 1}{X - m_D\, \alpha/2} - \exp\left[\frac{m_D}{2\mu}\left(e^{-2\mu T_\alpha} - 1\right)\right] \; \frac{e^{X T_\alpha}}{X},$$

and using the definition of $T_\alpha = \frac{1}{2\mu} \ln \frac{2}{\alpha}$, we obtain

$$\int_0^\infty f(t)dt \leq -\left(\frac{\alpha}{2}\right)^{\frac{-X}{2\mu}} \left[\frac{\gamma}{X - \alpha\, m_D/2} + \frac{\rho}{X}\right],$$

with $\gamma := \left(\frac{\alpha}{2}\right)^{\frac{X}{2\mu}} - \left(\frac{\alpha}{2}\right)^{\alpha m_D/(4\mu)}$ and $\rho = \exp\left[\frac{m_D}{2\mu}\left(\frac{\alpha}{2} - 1\right)\right]$. This leads to the following inequality:

$$\overline{r}(\infty) = -\; \frac{1}{\int_0^\infty f(t)dt} \leq \left(\frac{\alpha}{2}\right)^{\frac{X}{2\mu}} \; \frac{X - \alpha m_D/2}{\gamma + \rho\, \left(1 - \frac{\alpha m_D}{2X}\right)},$$

which can be rewritten:

$$\overline{r}(\infty) \leq \frac{X - \alpha m_D/2}{1 + \varepsilon},$$

with

$$\varepsilon := \left(1 - \frac{\alpha\, m_D}{2\, X}\right) \rho\, \left(\frac{\alpha}{2}\right)^{-\frac{X}{2\,\mu}} - \left(\frac{\alpha}{2}\right)^{\frac{\alpha\, m_D}{4\,\mu} - \frac{X}{2\,\mu}}.$$

Next, to show that $\overline{r}(\infty) < X - \alpha m_D/2$, we only need to check that $\varepsilon < 0$. This is true for certain values of α. As $\rho = \exp\left[\frac{m_D}{2\mu}\left(\frac{\alpha}{2} - 1\right)\right]$, we observe that ε has the same sign as:

$$\varepsilon' = \left(1 - \frac{\alpha\, m_D}{2\, X}\right) \exp\left[\frac{m_D}{4\,\mu}(\alpha - 2)\right] - \exp\left[\frac{m_D}{4\,\mu}\alpha\, \ln(\alpha/2)\right].$$

Since $X = r_{\max} - \mu n/2$, we get:

$$\varepsilon' = \frac{m_D}{4\,\mu}\left[-\alpha\, \ln(\alpha/2) + \alpha\,(1 + 4/n) - 2\right] + o\left(\frac{1}{\mu}\right),$$

as $\mu \to \infty$. Thus, $\varepsilon < 0$ for μ large enough, if and only if:

$$n > \frac{4}{\ln(\alpha/2) - 1 + 2/\alpha}. \tag{A10}$$

For α small enough, this inequality is true for any $n \geq 1$. However, higher values of α lead to sharper estimates of $\delta(m_D)$ in (8). With $\alpha = 1/4$ for instance, the inequality (A10) is always satisfied (as $n \geq 1$). We obtain that $\overline{r}(\infty) \leq X - \frac{m_D}{8}$ and $\delta(m_D) \geq \frac{m_D}{8}$ for μ large enough. If α is increased, e.g., $\alpha = 1/2$, the inequality (A10) is true for all $n \geq 3$, and consequently, $\overline{r}(\infty) \leq X - \frac{m_D}{4}$ for μ large enough ($\delta(m_D) \geq \frac{m_D}{4}$, for μ large enough). In our numerical computations ($n = 6$), we can use $\alpha = 3/4$, which leads to $\overline{r}(\infty) \leq X - \frac{3\,m_D}{8}$ and $\delta(m_D) \geq \frac{3\,m_D}{8}$ for large μ.

J Establishment time t_0: formula (9)

We recall that t_0 is defined as the first zero of $\overline{r}(t)$. We note that, since $\overline{r}(t)$ is increasing, it admits at most one zero.

First, if $r_{\max} - \mu n/2 \leq 0$, as $\overline{r}(t)$ is increasing and $\overline{r}(\infty) < r_{\max} - \mu\, n/2$ (see (8) and Appendix I), we have $\overline{r}(t) < 0$ for all $t \geq 0$. This implies that $t_0 = \infty$.

Second we assume that $r_{\max} - \mu n/2 > 0$. In this case, $\overline{r}(\infty) = r_{\max} - \mu n/2 > 0$ and the time t_0 is finite (and positive). Therefore, we can solve the equation $\overline{r}(t) = 0$, which is equivalent to:

$$(r_{\max} - \mu n/2)t + \frac{m_D}{2\mu}\left(e^{-2\mu t} - 1\right) = 0. \tag{A11}$$

Let us set $c := m_D/(r_{\max} - \mu\, n/2)$. Since $\overline{r}(0) = r_{\max} - \mu\, n/2 - m_D < 0$, we observe that $c > 1$. The equation (A11) is equivalent to:

$$2\mu\, t - c = -c\, e^{-2\,\mu\, t}.$$

Multiplying this expression by $e^{2\mu\, t - c}$, we get:

$$(2\mu\, t - c)e^{2\mu\, t - c} = -c\, e^{-c}.$$

Setting $X := 2\mu\, t - c$, we obtain:

$$X\, e^{X} = -c\, e^{-c}. \tag{A12}$$

As $c > 1$, $-ce^{-c} \in (-e^{-1}, 0)$, thus the equation (A12) admits two solutions, $X_0 = W_0(-c\, e^{-c})$ and $X_{-1} = W_{-1}(-c\, e^{-c}) < X_0$, with W_0 and W_{-1} respectively the principal branch and the lower branch of the Lambert-W function. Thus, the equation (A11) admits two solutions, $(c + X_0)/(2\mu)$ and $(c + X_{-1})/(2\mu) = 0$, but only the first one is positive. Finally, we obtain that

$$t_0 = \frac{1}{2\mu}\left(c + W_0(-ce^{-c})\right). \tag{A13}$$

As t_0 is an increasing function of c, we obtain that t_0 decreases as $r_{\max}$ is increased, and t_0 increases as m_D and n are increased. The dependence with respect to μ is more subtle. Differentiating the expression (A13) with respect to μ, we observe that $t_0'(\mu)$ has the same sign as:

$$\left(\frac{\mu\, n}{2\, r_{\max} - \mu\, n} - 1 - W_0(-ce^{-c})\right)\left(c + W_0(-ce^{-c})\right).$$

As the second factor in the above expression is always positive (since $c > 1$), we get that $t_0'(\mu)$ has the same sign as the function:

$$g(\mu) := \frac{\mu\, n}{2\, r_{\max} - \mu\, n} - 1 - W_0(-ce^{-c}).$$

Differentiating g with respect to μ, we observe that $g'(\mu)$ has the same sign as $r_{\max} + (\mu\, n/2 + m_D)\, W_0(-ce^{-c}) = r_{\max} - \mu\, n/2 + \mu\, n\, (1 - W_0(-ce^{-c}))/2 + m_D\, W_0(-ce^{-c})$. Thus $g'(\mu)$ has the same sign as $m_D\, (1/c + W_0(-ce^{-c})) + \mu\, n(1 - W_0(-ce^{-c}))/2 > 0$, as $1/c + W_0(-ce^{-c}) > 0$ (since $c > 1$) and $1 - W_0(-ce^{-c}) > 0$. Finally, g is increasing, with:

$$g(0) = -1 - W_0\left(-\frac{m_D}{r_{\max}} e^{-\frac{m_D}{r_{\max}}}\right) \leq 0,$$

(and the sign is strict unless $m_D = r_{\max}$). Additionally, we have $g(2r_{\max}/n) = +\infty$ (corresponding to μ_{lethal}). This means that, unless $m_D = r_{\max}$, $t_0(\mu)$ first decreases until μ reaches an optimal value, and then increases as μ is increased.

K Establishment time t_0: dependence with the habitat difference m_D and the immigration rate d

Using the stochastic individual-based model of Section 2.5, we analyzed the dependence of the establishment time t_0 with respect to m_D and d for a wide range of parameter values. Namely, taking $U = 0.1$, $r_{\max} = 0.1$, $\lambda = 1/300$ and $n = 6$ as in Fig. 6, m_D was varied between 0.1 and 0.5. The results are presented in Fig. A3a. It shows that, for each value of m_D, there is a threshold value of the immigration rate above which the establishment time t_0 becomes almost independent of d. This threshold tends to increase as the habitat difference m_D takes higher values. Additionally, we measured the relative error between the theoretical value of t_0 given by formula (9) and the value given by individual-based simulations; see Fig. A3b. As soon as the parameters are far from the black region in Fig. A3, (a,b), the approximation is good (relative error < 0.1). This black region corresponds to values of $t_0 > 5000$, for which individual-based simulations were stopped before establishment, and where we can expect that the final outcome is establishment failure. This means that there is only a narrow region where formula (9) is not accurate; it is located close to the region where establishment fails, and describes a rapid increase in t_0 which is not captured by our analytical approach.

Fig. A3 (c,d) depicts comparable simulations, with $U = U_c/3 = 0.01$, i.e., outside of the WSSM regime. The conclusions are similar to the case $U = 0.1$, but with a larger region corresponding to establishment failure, and a lower accuracy (panel d).

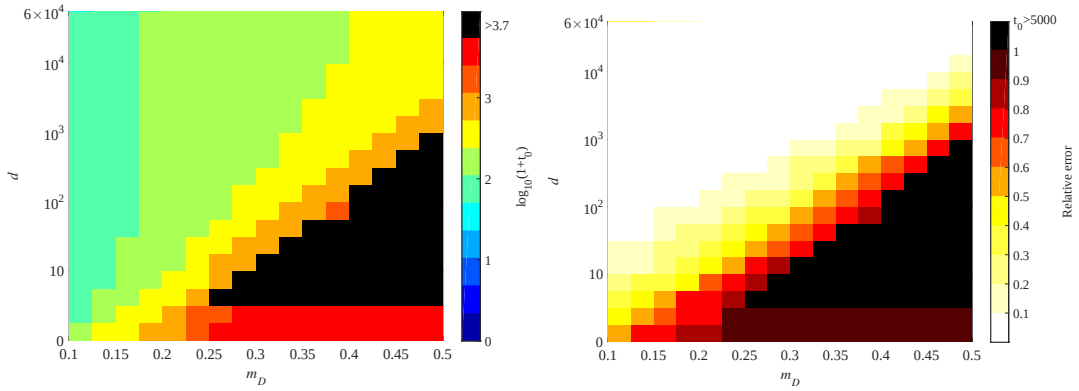

(a) $U = 0.1$ Establishment time

(b) $U = 0.1$ Relative error

(c) $U = 0.01$, establishment time

(d) $U = 0.01$, relative error

Figure A3: **Establishment time t_0, dependence with the habitat difference m_D and the immigration rate d.** (a,c): Average value of t_0 over 100 individual-based simulations. The color legend corresponds to $\log_{10}(1+t_0)$. (b,d): relative error between the theoretical value of t_0 given by formula (9) and the average value obtained by individual-based simulations. The black regions correspond to parameter values for which at least one simulation led to $t_0 > 5000$; in that case, the average value of t_0 was not computed numerically. In all cases, the parameter values are $r_{\max} = 0.1$, $\lambda = 1/300$, $n = 6$.

L Dynamics in the absence of mutation in the sink

We have seen in Fig 6b that mutation has a non-monotonic impact on establishment time. However, a higher mutation rate affects both the source equilibrium state and the sink dynamics. A natural question to ask is thus whether local mutation *in the sink* helps or hinders invasion. Indeed, mutation in the FGM (and other models with both deleterious and beneficial mutations) can have antagonistic effects: it generates fitness variance to fuel adaptation but lowers the mean fitness by creating a mutation load. This is of course also true for mutation in the source, but the interaction with migration in the sink makes the outcome less straightforward to grasp.

To tell apart the influences of local mutation on invasion speed, we analyze a scenario where mutation is absent in the sink, but still active in the source, so that the latter is unchanged. Using the same arguments as in Appendix D, we can derive a formula for $\overline{r}(t)$ in that case. The formula can be expressed in the same form as (7), with:

$$f(t) = \exp\left[\phi(t) + r_{\max}\, t\right],$$

with ϕ given by (3). We compared the corresponding time to establishment, noted t_0^0, with the establishment time t_0 to check whether local mutation (in the sink) speeds or slows invasion.

The results in Fig. A4 show that local mutation can either slow down or accelerate invasion, depending on the mutational variance (μ) and habitat difference (m_D). For a given level of m_D, local mutation tends to speed invasion as long as mutational variance (μ) is limited (left part of the graph) but hinders it when it becomes larger (right part of the graph). The transition from helping to hindering invasion happens at larger μ values when m_D is larger. It thus appears that the beneficial effect of local mutation in producing variance dominates when mutation is limited while its negative effect in load buildup takes over as μ is increased. The transition occurs at higher μ under higher m_D because the former effect is more critical then, while the latter is roughly independent of m_D. This pattern illustrates quite strikingly the complex implications, for adaptation dynamics, of the ambivalent nature of mutation in the FGM.

An example of trajectory of fitness is given in Fig. A5, where we observe that the four phases are still present. The corresponding phenotype distribution is presented in Fig. A6. A video file of the phenotype distribution is also available as Supplementary File 3.

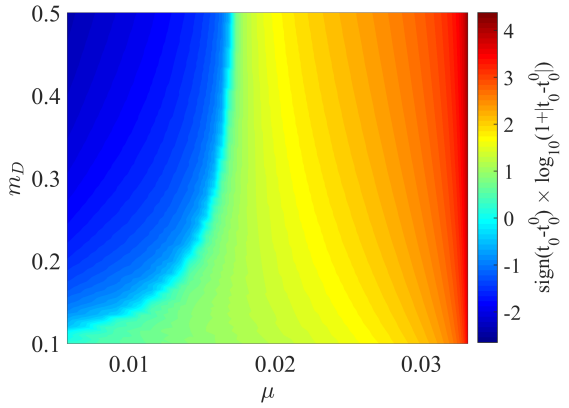

Figure A4: **Comparison between the establishment times t_0 (with mutation in the sink) and t_0^0 (without mutation in the sink).** The heat map corresponds to $\mathrm{sign}(t_0 - t_0^0)\ \log_{10}(1+|t_0-t_0^0|)$: negative values indicate that $t_0^0 > t_0$ (faster establishment with mutation in the sink) and positive values indicate that $t_0 > t_0^0$ (faster establishment without mutation in the sink).

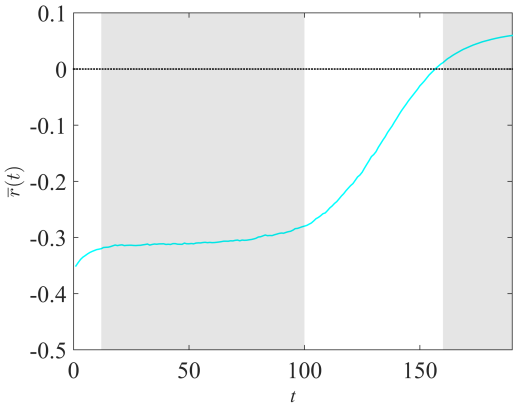

Figure A5: **Dynamics of $\overline{r}(t)$ in the absence of mutation in the sink.** The blue curve corresponds to the trajectory of $\overline{r}(t)$ given by a single individual-based simulation, in the absence of mutation in the sink. The parameter values are $m_D = 0.4$, $U = 0.1$, $r_{\max} = 0.1$, $\lambda = 1/300$, $n = 6$ and $d = 10^4$.

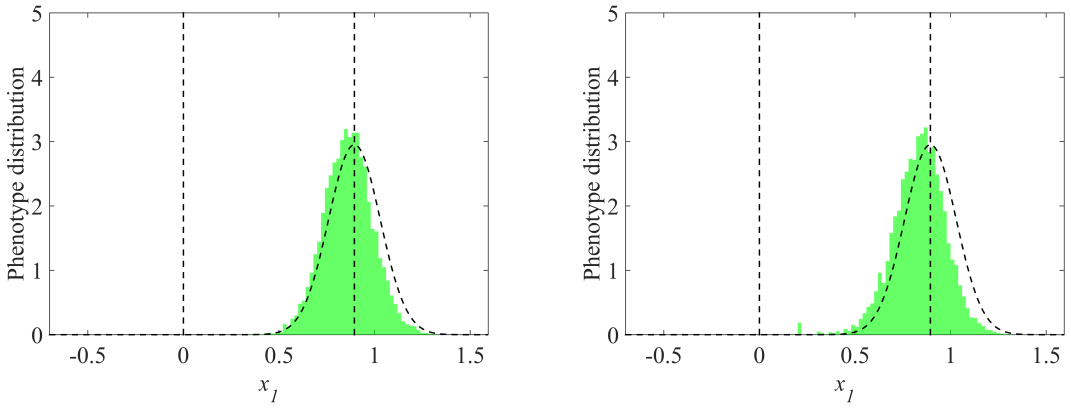

(a) Phase 1: $t = 10$

(b) Phase 2: $t = 50$

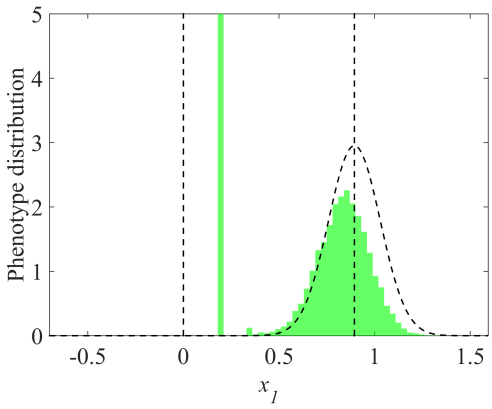

(c) Phase 3: $t = 115$

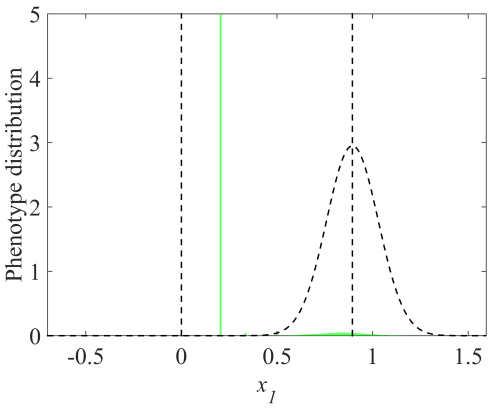

(d) Phase 4: $t = 190$

Figure A6: **Phenotype distribution in the sink, along the direction x_1, in the absence of mutation.** The vertical dotted lines correspond to the sink ($x_1 = 0$) and source ($x_1 = \sqrt{2\,m_D}$) optima. The black dotted curve corresponds to the theoretical distribution of migrant's phenotypes in the sink (Gaussian distribution, centered at $x_1 = \sqrt{2\,m_D}$, and with variance $\mu = \sqrt{U\,\lambda}$). The parameter values are $m_D = 0.4$, $U = 0.1$, $r_{\max} = 0.1$, $\lambda = 1/300$, $n = 6$ and $d = 10^4$.

References

Kimura, M. (1965). A stochastic model concerning the maintenance of genetic variability in quantitative characters. *Proceedings of the National Academy of Sciences 54*(3), 731–736.

Lande, R. (1980). The genetic covariance between characters maintained by pleiotropic mutations. *Genetics 94*(1), 203–215.

Martin, G. (2014). Fisher's geometrical model emerges as a property of complex integrated phenotypic networks. *Genetics 197*(1), 237–255.

Martin, G. and T. Lenormand (2015). The fitness effect of mutations across environments: Fisher's geometrical model with multiple optima. *Evolution 69*(6), 1433–1447.

Martin, G. and L. Roques (2016). The non-stationary dynamics of fitness distributions: Asexual model with epistasis and standing variation. *Genetics 204*(4), 1541–1558.

Tenaillon, O. (2014). The utility of Fisher's geometric model in evolutionary genetics. *Annual Review of Ecology, Evolution, and Systematics 45*, 179–201.

Trindade, S., L. Perfeito, and I. Gordo (2010). Rate and effects of spontaneous mutations that affect fitness in mutator Escherichia coli. *Philosophical Transactions of the Royal Society B: Biological Sciences 365*(1544), 1177–1186.